# Chemisorption of acetonitrile, pyridine and pyrazine on the Si(100)-2×1 surface: theoretical predictions

**Xin Lu,\* Xin Xu, Jianming Wu, Nanqin Wang and Qianer Zhang**

*State Key Laboratory for Physical Chemistry of Solid Surfaces, Institute of Physical Chemistry, Department of Chemistry, Xiamen University, Xiamen 361005, China. E-mail: xinlu@xmu.edu.cn; Fax: +86 592 218 3047; Tel: +86 592 218 1600*

The chemisorption of acetonitrile ($CH_3CN$), pyridine ($C_5H_5N$) and pyrazine ($C_4H_4N_2$) on the Si(100)-2×1 surface has been investigated by means of first-principles density functional cluster model calculations. For acetonitrile, an N-end-on adsorption state and a side-on adsorption state were found, together with a transition state that connects the two adsorption states. The predicted energetics suggests that the side-on adsorption state can be readily formed at rather low temperature *via* the end-on precursor state. For both pyridine and pyrazine, an N-end-on adsorption state and two side-on adsorption states were revealed. In the pyridine/Si(100) chemisorption system, the primary adspecies would be the N-end-on adsorbed pyridine as the N-end-on adsorption is the most favorable and barrierless. For the pyrazine case, the N-end-on adsorbed pyrazine would be the primary adspecies at low temperature, while at elevated temperatures the primary adspecies would be the side-on adsorbed pyrazine, which is di-σ bonded onto the surface dimer through the 2 and 5 carbon atoms. In particular, the finding that the N-end-on adsorption of pyridine on the Si(100)-2×1 surface is substantial enlightens us as to the possibility of constructing a pyridine-based, conductive (or semiconductive) polymer film on the Si surface.

The chemistry of organic molecules on Si surfaces is not only of fundamental interest, but also of practical importance.[1,2] Small organic molecules on Si surfaces serve as model systems for studies of the process of SiC, SiN, SiCN and thin diamond film formation on surfaces.[1–6] Accordingly, a large number of experimental and theoretical studies have been reported on this topic in the past decade.[1–35] Most of them concerned the chemistry of alkanes, alkenes,[1–17] alcohols[18–23] and simple aromatic compounds[15,24–32] on silicon surfaces. We have recently performed a series of theoretical investigations regarding the chemisorption of methanol,[23] formaldehyde,[23] formic acid,[23] acetonitrile, thiophene,[31,32] furan,[31,32] pyridine and some other aromatic compounds[32] on the reconstructed Si(100)-2×1 surface. In this paper, we present theoretical predictions of the chemisorption of acetonitrile ($CH_3CN$), pyridine ($C_5H_5N$) and pyrazine ($C_4H_4N_2$) on the Si(100)-2×1 surface based on first-principles density functional cluster model calculations.

No experimental work has so far been reported regarding the chemisorption of $CH_3CN$ on the Si(100)-2×1 surface. Acetonitrile is a polar molecule with a dipole moment of 3.92 D.[33] A recent scanning tunneling microscope (STM) study revealed that at low temperature (∼120 K), $CH_3CN$ adsorbs across the dimer row of the Si(111)-7×7 surface, probably due to the dipole–dipole interaction between the polar molecule and the Si(111)-7×7 surface.[34] The Si(100)-2×1 surface, however, adopts a rather different bonding motif from the Si(111)-7×7 surface, in that the adjacent surface Si atoms on the Si(100) surface are paired up to form dimers.[1,35] The bonding within the surface dimer can be described in terms of a strong σ bond and a rather weaker π bond; the surface dimer, to some extent, acts as a diradical.[35] Previous experimental and theoretical studies revealed that the surface dimer is highly reactive toward simple alkenes, dienes and other molecules containing double or triple bonds, forming [2+2] cycloaddition-like surface species;[35,36] this [2+2] cycloaddition-like chemisorption follows an asymmetric pathway.[35] It is thus deducible that the chemisorptive behavior of $CH_3CN$ on the Si(100)-2×1 surface would be closely related to the high reactivity of the surface dimer and the –C≡N group, which contains a triple bond. One purpose of the present study is to verify the above inference theoretically.

The adsorption of pyridine on Si(111) surfaces has been studied experimentally,[25,34] but none concerns the adsorption of pyridine on the Si(100) surface to date. Pyridine is a six-membered aromatic ring compound with an N heteroatom. The lone pair on the N atom induces a dipole moment of 2.19 D.[33] A recent STM study suggested a dipole–dipole interaction between pyridine and the Si(111)-7×7 surface, that is the interaction is electrostatic, not chemical, in nature.[34] It is uncertain whether pyridine would display different adsorption behavior on the structurally different Si(100)-2×1 surface. For another aromatic compound, benzene, recent experiments and theoretical investigations revealed that its chemisorption on the Si(100)-2×1 surface follows the famous Diels–Alder cycloaddition mechanism, giving rise to a di-σ bonded, 1,4-cyclohexadiene-like adspecies.[28,30,32] Pyridine is isoelectronic with benzene, and may follow a similar chemisoption mechanism. However, it is known that the lone pair on the N heteroatom endows pyridine with different bonding modes than benzene when interacting with a transition metal atom (TM).[37] For example, pyridine can form an N–TM σ bond with a transition metal atom, while no similar σ bond can be formed in a benzene-TM complex without breaking a C–H bond.[37] The second objective of the present study is to investigate in which ways the heteroatom(s) would influence the chemisorption behavior of the 6-membered aromatic ring

compounds on the Si(100)-2×1 surface. For this purpose, the chemisorption of pyridine and pyrazine has been studied theoretically.

## Computational details

The Si(100) surface adopts a (2×1) reconstruction and the adjacent surface atoms pair into dimers, as shown in Fig. 1(a). A $Si_9H_{12}$ cluster model [Fig. 1(b)] has been used to represent the reconstructed Si(100)-2×1 surface. Its top layer consists of two Si atoms forming a Si–Si dimer. Despite its simplicity in that it neglects the interaction among adjacent dimers, this cluster model has been shown to give reasonable energetic and geometric predictions for chemisorption and reaction on the Si(100)-2×1 surface.[12,15,16,23,29–32,36]

All calculations were performed with the GAUSSIAN94 package.[38] The hybrid density functional method including Becke's 3-parameter nonlocal-exchange functional[39] with the correlation functional of Lee–Yang–Parr[40] (B3LYP) was employed. The basis set used is the standard 6-31G(d) basis set.[41] For all the stationary points (local minima and transition states) concerned, geometry optimizations and vibrational analyses were performed using the Berny algorithm without any constraints on the degrees of freedom. Each of the calculated transition states has been found to have one imaginary frequency. Connectivity of the stationary points (transition states and adjacent local minima) along the reaction paths has been confirmed by intrinsic reaction coordinate (IRC) calculations.[42] Unscaled zero-point energies (ZPE) were also evaluated at the B3LYP/6-31G(d) level of theory. Reported energetics are ZPE-corrected, unless otherwise specified. Reported frequencies are scaled by 0.96.

## Results and discussion

### $CH_3CN/Si_9H_{12}$ model system

For $CH_3CN$ adsorbed on the $Si_9H_{12}$ surface model, two local minima as well as a transition state that connects the two local minima have been located in our calculations at the B3LYP/6-31G(d) level of theory. The optimized geometries of these stationary points are given in Fig. 2. The profile of the energy surface is depicted in Fig. 3.

As shown in Fig. 2, the first local minimum, LM_1, is a molecular adsorption state, in which $CH_3CN$ adopts an end-on configuration with its N-end on top of the buckled-down Si atom of the surface dimer. The geometry of $CH_3CN$ adspecies changed slightly from that of free $CH_3CN$. In free $CH_3CN$, the angle ∠CCN and the C–C and C≡N bond lengths are 180°, 1.462 and 1.160 Å, respectively, whereas in adsorbed $CH_3CN$ the three key parameters are 179.7°, 1.453 and 1.158 Å, respectively. The intermolecular Si–N distance is 1.892 Å. The formation of LM_1 from free $CH_3CN$ is barrierless and is initiated by a nucleophilic attack of the negatively charged
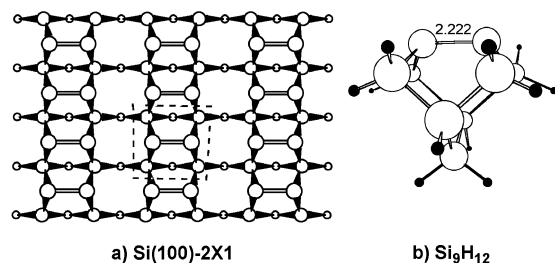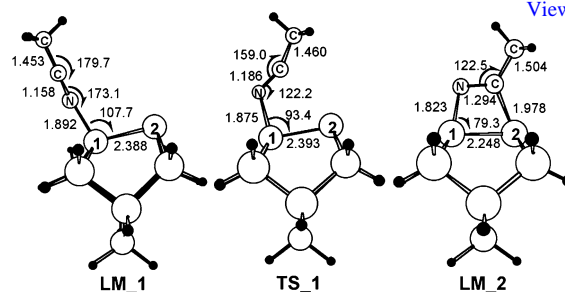


**Fig. 2** Local minima and transition state for the $CH_3CN/Si_9H_{12}$ model system predicted at the B3LYP/6-31G(d) level of theory.

N-end of $CH_3CN$ toward the buckled-down Si atom, which is positively charged.[35] The exothermicity predicted for the formation of LM_1 from free $CH_3CN$ is −15.8 (−16.6) kcal mol$^{-1}$ with (without) ZPE correction at the B3LYP/6-31G(d) level. NBO (natural bond orbital) analysis[43] of the Kohn–Sham wavefunctions of the model system reveals a N–Si-(buckled-down) σ bond formed between the lone pair on the N atom and the empty, anti-bonding orbital localized on the Si dimer. The contribution to the N–Si(buckled-down) σ bond is 85% from the lone pair on the N atom and 15% from the dangling bond of the buckled-down Si atom. Such dative bonding results in a positively charged $CH_3CN$ adspecies (with a natural charge of +0.16 au) as well as an elongation (by ~0.166 Å) of the Si–Si bond. A similar molecular adsorption state was found in a previous DFT study of HCN adsorption on the same surface.[36]

In another local minimum (LM_2), $CH_3CN$ adopts a side-on configuration with its –CN group di-σ bonded onto the Si–Si dimer. The formation of LM_2 is exothermic by −27.8 (−29.6) kcal mol$^{-1}$ predicted at the B3LYP/6-31G(d) level with (without) ZPE correction. Hence, the side-on adsorption of $CH_3CN$ is thermodynamically favorable over the end-on adsorption. The thus-formed C–Si and N–Si bond lengths are 1.978 and 1.823 Å, respectively. Meanwhile, the C=N and Si–Si bond lengths are elongated by 0.134 and 0.026 Å, respectively, with respect to those (1.160 and 2.222 Å) in free $CH_3CN$ and $Si_9H_{12}$. As such, LM_2 can be regarded as a result of the [2 + 2] cycloaddition between the –C≡N group and the surface dimer. Similar [2 + 2] cycloaddition-like chemisorptions have been previously revealed on the Si(100)-2×1 surface for the chemisorption of molecules containing double or triple bonds, including C=C in $C_2H_4$,[7–9,35] C≡C in
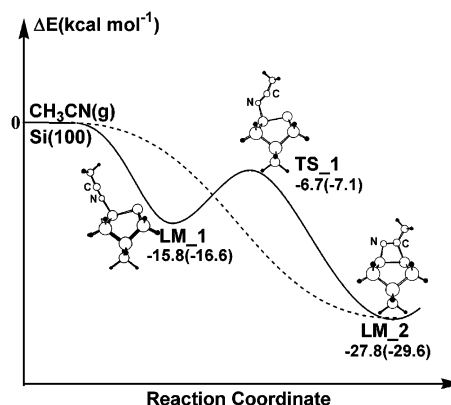


**Fig. 1** (a) Top view of the reconstructed Si(100)-2×1 surface and (b) the $C_9H_{12}$ cluster model.



**Fig. 3** Profile of the energy surface for the $CH_3CN/Si_9H_{12}$ model system predicted at the B3LYP/6-31G(d) level of theory. ZPE-uncorrected values are given in parentheses. The solid line indicates the indirect formation of the di-σ bonded adspecies (LM_2), while the dashed line shows the direct formation of LM_2.

$C_2H_2$,[11–13,35] C=O in $CH_2O$[23] and biacetyl,[44] N=N in azo-*tert*-butane,[45] C=N in phenyl isothiocyanate,[46] and C≡N in HCN.[36]

Further efforts have been made to verify if there is a transition state between free $CH_3CN$ and the side-on adsorption state. But no such transition state has been found. Instead, we found a transition state (TS_1) that connects the thermodynamically favorable side-on adsorption state (LM_2) and the weaker, end-on adsorption state (LM_1). As shown in Fig. 3, the barrier height for the end-on to side-on transformation is 9.1 kcal mol$^{-1}$ as predicted at the B3LYP/6-31G(d) level. However, the prediction that TS_1 is 6.7 kcal mol$^{-1}$ lower in energy than the initial reactants suggests that the side-on chemisorption state can be readily formed *via* a precursor state, that is LM_1, at low temperature. As such, whether the direct formation of the side-on chemisorption state from free $CH_3CN$ is barrierless or not is not important.

The calculated vibrational frequencies for the end-on and side-on adsorbed $CH_3CN$ and free $CH_3CN$ are listed in Table 1, together with the experimental data[47] for free $CH_3CN$. Unfortunately, no experimental datum is available for the $CH_3CN$/Si(100) chemisorption system. Nevertheless, the theoretical data given in Table 1 shall be informative for future experimental study of this system by means of vibrational spectroscopy.

## $C_5H_5N$/$Si_9H_{12}$ model system

For $C_5H_5N$ on the $Si_9H_{12}$ surface model, three local minima have been obtained in our calculations. The optimized geometries and the relative energies of these stationary points are given in Fig. 4.

In the first local minimum (LM1), $C_5H_5N$ adopts an end-on configuration with its N-end on top of the buckled-down Si atom of the surface dimer and its molecular plane parallel with the normal of the Si(100) surface. The exothermicity predicted for the formation of LM1 from free $C_5H_5N$ is $-27.0$ ($-28.4$) kcal mol$^{-1}$ at the B3LYP/6-31G(d) level after (before) ZPE correction. Such an end-on chemisorption is barrierless through a nucleophilic attack of the negatively charged N atom toward the positively charged, buckled-down Si atom of the surface dimer. The N–Si(buckled-down) bond with an optimal length of 1.976 Å is formed due to dative bonding between the lone pair on the N atom of pyridine and the empty, anti-bonding orbital of the surface dimer, which is mostly localized on the buckled-down Si atom. This bonding scheme is confirmed by NBO analysis of the wavefunctions of the model system, which indicates that the occupancy of the donor NBO on the N atom is only 1.73 au and the occupancy of the acceptor NBO on the buckled-down Si atom is 0.45 au. As a result, pyridine is positively charged with a natural charge
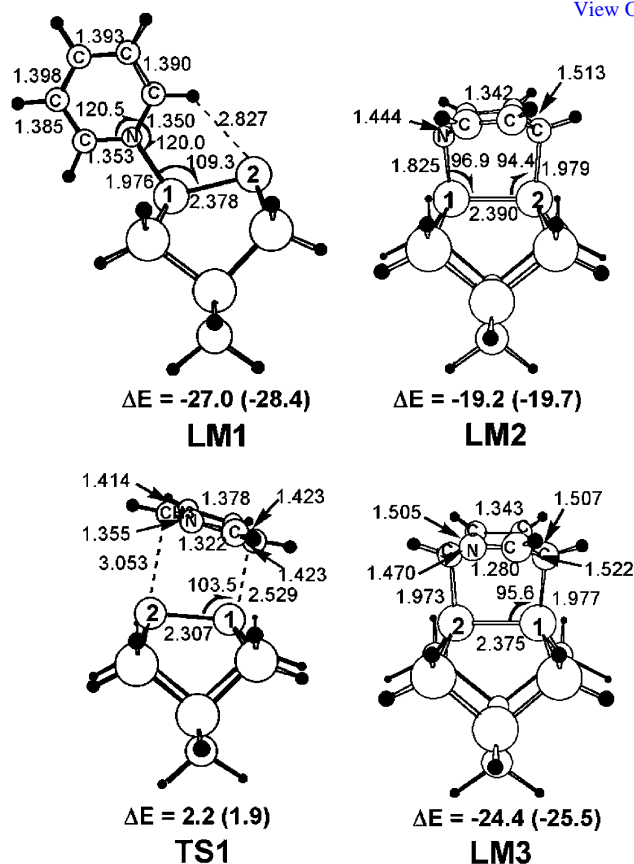


**Fig. 4** Local minima and transition state for the $C_5H_5N$/$Si_9H_{12}$ model system predicted at the B3LYP/6-31G(d) level of theory. The relative energies ($\Delta E$/kcal mol$^{-1}$) of these stationary points with respect to free $C_5H_5N$ are also given, together with the ZPE-uncorrected data in parentheses.

of $+0.24$ au and the Si–Si bond length in the surface dimer is elongated by 0.156 Å upon the N-end-on chemisorption of pyridine. Furthermore, it is noteworthy that for the end-on adsorption of $CH_3CN$ and pyridine on the Si(100)-2×1 surface, the larger exothermicity in the pyridine case than in that of the acetonitrile case suggests that the lone pair on the N atom of pyridine is more donative than that of $CH_3CN$.

Apart from the end-on adsorption state, two side-on adsorption states (LM2 and LM3) were also found, as depicted in Fig. 4. LM2 is bonded onto the surface dimer through its 1 and 4 positions involving the heteroatom and a C atom, while LM3 is bonded through its 2 and 5 positions involving two C atoms. The thus-formed adspecies are both butterfly-like. The formation energy of LM3 is $-24.4$ kcal mol$^{-1}$, larger than that of LM2 ($-19.2$ kcal mol$^{-1}$), but smaller than that of LM1 ($-27.0$ kcal mol$^{-1}$). However, the formation of the thermodynamically favorable LM3 is kinetically less favorable than the formation of LM2. At the B3LYP/6-31G(d) level, a transition state (TS1) has been located that connects free pyridine and LM3; the barrier height for the formation of LM3 from free pyridine is 2.2 kcal mol$^{-1}$, while the formation of LM2 is found to be barrierless.

The formation of the two side-on states follows the so-called [4 + 2] cycloaddition mechanism, as previously revealed for the chemisorption of benzene on the Si(100)-2×1 surface.[15,30,32] The LUMO (lowest unoccupied molecular orbital) of the aromatic compounds and the HOMO (highest occupied molecular orbital) of the surface dimer are the primary frontier orbitals involved in the [4 + 2] cycloaddition process.[15,30] Accordingly, it can be conjectured that the direction of charge transfer would be from the surface to the adspecies during the cycloaddition process. This is confirmed by the results of

**Table 1** B3LYP/6-31G(d) calculated vibrational frequencies (cm$^{-1}$) for free and chemisorbed $CH_3CN$ and experimental data for free $CH_3CN$

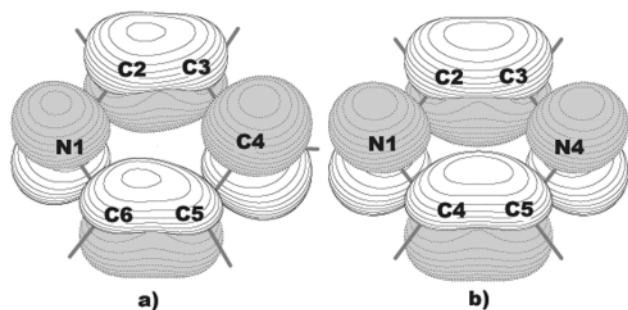| Mode | Free $CH_3CN$ | | $CH_3CN$/Si(100) | |
|---|---|---|---|---|
| | Calcd | Exptal[a] | End-on | Side-on |
| C–H str | 3015(2) | 3009(2) | 3020, 3018 | 3012, 2972 |
| | 2945 | 2954 | 2942 | 2916 |
| C≡N str | 2282 | 2267 | 2281 | |
| C=N str | | | | 1524 |
| C–H bend | 1442(2) | 1448(2) | 1425, 1424 | 1438, 1428 |
| | 1382 | 1383 | 1372 | 1356 |
| $CH_3$ rock | 1034(2) | 1041(2) | 1022, 1019 | 1098, 988 |
| C–C str | 926 | 920 | 924 | 948 |

[a] Ref. 47.

**Fig. 5** Contour of frontier orbitals: (a) LUMO of pyridine, (b) LUMO of pyrazine.

Mulliken population analysis that the charges on the adspecies in LM2 and in LM3 are $-0.39$ and $-0.32$ au, respectively. Fig. 5(a) depicts the contour of the LUMO of free pyridine, which shows why the [4 + 2] cycloaddition of pyridine onto the surface dimer can proceed through either the 1,4 or the 2,5 positions of the pyridine ring.

Conclusively, the predicted energetics suggest that the primary adspecies in the pyridine/Si(100) chemisorption system would be the end-on adsorbed pyridine. This finding should be significant for the development of pyridine-based, conductive polymer films on silicon surfaces, as the pyridine-surface bonding is substantial and, most importantly, does not involve the $\pi$ states of the conjugated system. It should be mentioned that the adsorption of other aromatic compounds, such as benzene, thiophene and furan, *etc.*, has been shown to inevitably destroy the $\pi$-conjugation of the aromatic compounds, since the adsorption follows the Diels–Alder cycloaddition mechanism. Destruction of the $\pi$-conjugation in aromatic compounds is highly undesirable for the formation of thin films of organic semiconductor polymers on silicon surfaces.[48,49]

### $C_4H_4N_2/Si_9H_{12}$ model system

Similar to the pyridine/Si$_9$H$_{12}$ model system, three local minima were located for the pyrazine/Si$_9$H$_{12}$ model system, including an N-end-on adsorption state (LM1') and two side-on adsorption states (LM2' and LM3'). In addition, a transition state (TS1') that connects free pyrazine and the side-on adsorption state (LM3') was also located. The optimized geometries and the relative energies of the local minima and transition state for the $C_4H_4N_2/Si_9H_{12}$ model system are presented in Fig. 6.

Despite the fact that pyrazine forms chemisorption states similar to the pyridine case, the energetics predicted for the pyrazine case are different from the pyridine case, due to the different number of heteroatoms. Firstly, the exothermicity predicted for the N-end-on adsorption (LM1') of pyrazine is $-18.6$ kcal mol$^{-1}$. That is, the binding energy of the N-end-on adsorbed pyrazine is by 8.4 kcal mol$^{-1}$ lower than that of pyridine. Note that pyrazine is nonpolar, while pyridine is dipolar. The difference in binding energy of the end-on adsorbed pyridine and pyrazine can be attributed to the larger electrostatic interaction between the adspecies and the surface dimer in the dipolar pyridine case than in the nonpolar pyrazine case. Secondly, the side-on adsorption state (LM2') of pyrazine, which invovles two N heteroatoms in the adsorbate–surface bonding, has an adsorption energy of $-13.4$ kcal mol$^{-1}$. This is 5.8 kcal mol$^{-1}$ less exothermic than that of LM2 in the pyridine case, which involves only one N heteroatom. This demonstrates that the N–Si $\sigma$ bonding is weaker than the C–Si $\sigma$ bonding. Thirdly, the side-on adsorption state (LM3') involving two C–Si $\sigma$ bonds is thermodynamically the most favorable for the pyrazine case, while the most favorable
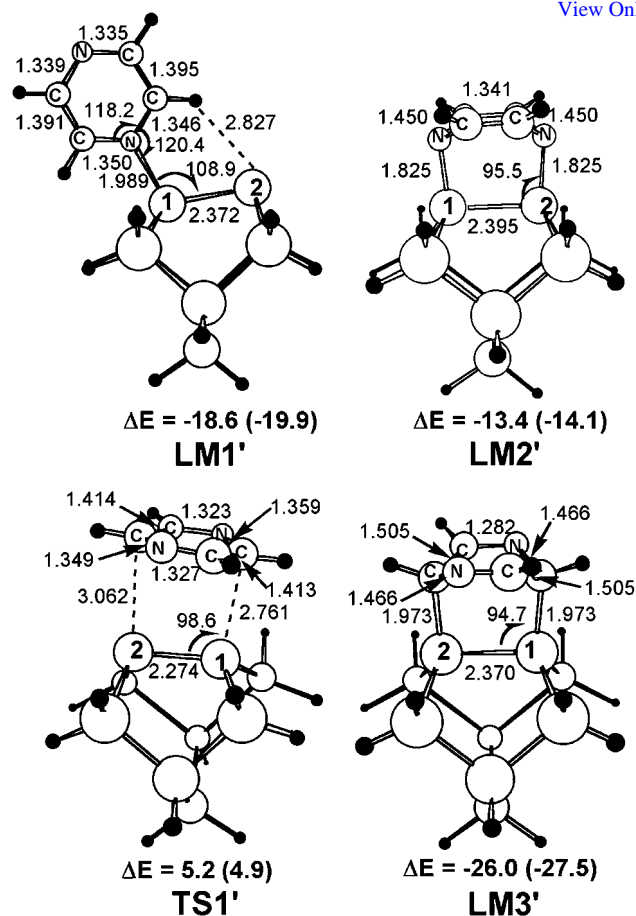


**Fig. 6** Local minima and transition state for the $C_4H_4N_2/Si_9H_{12}$ model system predicted at the B3LYP/6-31G(d) level of theory. The relative energies ($\Delta E$/kcal mol$^{-1}$) of these stationary points with respect to free $C_4H_4N_2$ are also given, together with the ZPE-uncorrected data in parentheses.

adsorption state for the pyridine case is the end-on adsorption state (LM1). Furthermore, the side-on adsorption LM3' has to overcome a low barrier of 5.2 kcal mol$^{-1}$ at the transition state (TS1'), while the end-on adsorption (LM1') and the side-on adsorption (LM2') are barrierless.

Fig. 5(b) depicts the contour of the LUMO of free pyrazine. This indicates that the side-on adsorption of pyrazine can occur through either its 1,4 N atoms or its 2,5 C atoms, following the Diels–Alder cycloaddition mechanism. Similar to the pyridine case, the side-on adsorbed pyrazine is negatively charged with a Mulliken charge of $-0.33$ au in LM2' and $-0.37$ au in LM3'.

Based on the predicted energetics, it can be concluded that in the pyrazine/Si(100) chemisorption system, the N-end-on adsorbed pyrazine would be the primary adspecies at low temperature, while at elevated temperatures the primary adspecies would be the side-on adsorbed pyrazine, which is di-$\sigma$ bonded onto the surface dimer through the 2,5 C atoms.

### Summary

The chemisorption of acetonitrile (CH$_3$CN), pyridine (C$_5$H$_5$N) and pyrazine (C$_4$H$_4$N$_2$) on the reconstructed Si(100)-2×1 surface has been investigated by means of the hybrid density functional B3LYP method in combination with a cluster model approach. For acetonitrile, an N-end-on adsorption state and a side-on adsorption state were found, together with a transition state that connects the two adsorption states. The predicted energetics suggests that the side-on, di-$\sigma$ bonded adsorption state can be readily formed at a rather low

temperature *via* the N-end-on precursor state. For both pyridine and pyrazine, an N-end-on adsorption state and two side-on adsorption states were revealed. For the pyridine case, the N-end-on adsorption is the most favorable and barrierless. For the pyrazine case, the N-end-on adsorbed pyrazine would be the primary adspecies at low temperature, while at elevated temperatures the primary adspecies would be the side-on adsorbed pyrazine, which is di-σ bonded onto the surface dimer through the 2,5 C atoms. Further experimental work is neccessary to confirm the theoretical predictions given above.

Finally, the finding that the N-end-on adsorption is the most favorable for pyridine on the Si(100)-2×1 surface enlightens us as to the possibility of constructing a pyridine-based, conductive (or semiconductive) polymer film on the Si(100)-2×1 surface.

## Acknowledgements

## References

1 H. N. Waltenburg and J. T. Yates, Jr., *Chem. Rev.*, 1995, **95**, 1589.
2 J. T. Yates, Jr., *Science*, 1998, **279**, 335.
3 A. J. Mayne, A. R. Avery, J. Knall, T. S. Jones, G. A. D. Briggs and W. H. Weinberg, *Surf. Sci.*, 1993, **289**, 247.
4 H. Gutleben, S. R. Lucas, C. C. Cheng, W. J. Choyke and J. T. Yates, Jr., *Surf. Sci.*, 1991, **257**, 146.
5 I. Kusunoki and Y. Igari, *Appl. Surf. Sci.*, 1992, **59**, 95.
6 K. P. Loh, C. R. Kingsley, J. S. Foord and R. B. Jackman, *Surf. Sci.*, 1995, **341**, 92.
7 P. A. Taylor, R. M. Wallace, C. C. Cheng, W. H. Weinberg, M. J. Dresser, W. J. Choyke and J. T. Yates, Jr., *J. Am. Chem. Soc.*, 1992, **114**, 6754.
8 H. Liu and R. J. Hamers, *J. Am. Chem. Soc.*, 1997, **119**, 7593.
9 H. Liu and R. J. Hamers, *Surf. Sci.*, 1998, **416**, 354.
10 G. P. Lopinski, D. J. Moffatt, D. D. M. Wayner and R. A. Wolkow, *J. Am. Chem. Soc.*, 2000, **122**, 3548.
11 S. H. Su, M. Keeffe, Y. Yang, C. Chen, M. Yu, G. J. Lapeyre, E. Rotenberg, J. Denlinger and J. T. Yates, Jr., *Phys. Rev. Lett.*, 2000, **84**, 939.
12 Q. Liu and R. Hoffmann, *J. Am. Chem. Soc.*, 1995, **117**, 4083.
13 Y. Imamura, Y. Morikawa, T. Yamasaki and H. Nakatsuji, *Surf. Sci. Lett.*, 1995, **341**, 1095.
14 A. J. Dyson and P. V. Smith, *Surf. Sci.*, 1997, **375**, 45.
15 R. Konecny and D. J. Doren, *Surf. Sci.*, 1998, **417**, 169.
16 C. H. Choi and M. S. Gordon, *J. Am. Chem. Soc.*, 1999, **121**, 11 311.
17 X. Lu and M. C. Lin, *Phys. Chem. Chem. Phys.*, 2000, **2**, 4213.
18 J. A. Glass, Jr., E. A. Wovchko and J. T. Yates, Jr., *Surf. Sci.*, 1995, **338**, 125.
19 J. Eng, Jr., K. Raghavachari, L. M. Struck, Y. J. Chabal, B. E. Bent, G. W. Flynn, S. B. Christman, E. E. Chaban, G. P. Williams, K. Rademacher and S. Mantl, *J. Chem. Phys.*, 1997, **106**, 9889.
20 M. P. Casaletto, R. Zanoni, M. Carbone, M. N. Piancastelli, L. Abelle, K. Weiss and K. Horn, *Surf. Sci.*, 2000, **447**, 237.
21 N. Y. Kim and P. E. Laibinis, *J. Am. Chem. Soc.*, 1997, **119**, 2297.
22 J. A. Stroscio, S. R. Bare and W. Ho, *Surf. Sci.*, 1985, **154**, 35.
23 X. Lu, Q. Zhang and M. C. Lin, *Phys. Chem. Chem. Phys.*, 2001, **3**, 2156.
24 M. Carbone, M. N. Piancastelli and L. Hellner, *Phys. Rev. B*, 2000, **61**, 8531; R. A. Wolkow and D. J. Moffatt, *J. Chem. Phys.*, 1995, **103**, 10 696; Y. Taguchi, M. Fujisawa and M. Nishijima, *Chem. Phys. Lett.*, 1991, **178**, 363.
25 M. N. Piancastelli, M. K. Kelly, G. Margaritondo, J. Anderson, D. J. Frankel and G. J. Lapeyre, *Phys. Rev. B*, 1985, **32**, 2351; C. D. MacPherson and K. T. Leung, *Surf. Sci.*, 1995, **324**, 202.
26 M. N. Piancastelli, M. K. Kelly, G. Margaritondo, D. J. Frankel and G. J. Lapeyre, *Surf. Sci.*, 1989, **211/212**, 1018; C. D. MacPherson, D.Q. Hu and K. T. Leung, *Surf. Sci.*, 1992, **276**, 156; S. Letarte, A. Adnot and A. Roy, *Surf. Sci.*, 2000, **448**, 212; Y. Cao, Z. Wang, J. F. Deng and G. Q. Xu, *Angew. Chem., Int. Ed.*, 2000, **39**, 2740.
27 M. N. Piancastelli, R. Zanoni, M. K. Kelly, D. G. Kilday, Y. Chang, J. T. McKinley, G. Margaritondo, P. Pertetti, C. Quaresima and M. Capozi, *Solid State Commun.*, 1987, **63**, 85; Y. Cao, K. S. Yong, Z. Q. Wang, W. S. Chin, Y. H. Lai, J. F. Deng and G. Q. Xu, *J. Am. Chem. Soc.*, 2000, **122**, 1812.
28 Y. Taguchi, M. Fujisawa, T. Takaoka, T. Okada and M. Nishijima, *J. Chem. Phys.*, 1991, **95**, 6870; G. P. Lopinski, T. M. Fortier, D. J. Moffatt and R. A. Wolkow, *J. Vac. Sci. Technol., A*, 1998, **16**, 1037; M. J. Kong, A. V. Teplyakov and S. F. Bent, *Surf. Sci.*, 1998, **411**, 286; S. K. Coutler, J. S. Hovis, M. D. Ellison and R. J. Hamers, *J. Vac. Sci. Technol., A*, 2000, **18**, 1965.
29 M. H. Qiao, Y. Cao, J. F. Deng and G. Q. Xu, *Chem. Phys. Lett.*, 2000, **325**, 508; H. Luo and M. C. Lin, *Chem. Phys. Lett.*, 2001, **343**, 219.
30 B. I. Craig, *Surf. Sci.*, 1993, **280**, L279; U. Birkenheuer, U. Gutdeutsch and N. Rösch, *Surf. Sci.*, 1998, **409**, 213; R. A. Wolkow, G. P. Lopinski and D. J. Moffatt, *Surf. Sci.*, 1998, **416**, L1107; P. L. Silvestrelli, F. Ancilotto and F. Toigo, *Phys. Rev. B*, 2000, **62**, 1596.
31 X. Lu, X. Xu, N. Wang, Q. Zhang and M. C. Lin, *J. Phys. Chem. B*, 2001, **105**, 10 069.
32 X. Lu, M. C. Lin, X. Xu, N. Wang and Q. Zhang, *Phys. Chem. Comm.*, 2001, 13.
33 *CRC Handbook of Chemistry and Physics*, ed. R. C. Weast, M. J. Astle and W. H. Beyer, Chemical Rubber Co., Boca Raton, FL, 66th edn., 1985, E58–E60.
34 N. Shirota, S. Yagi, M. Taniguchi and E. Hashimoto, *J. Vac. Sci. Technol., A*, 2000, **18**, 2578.
35 R. J. Hamers, S. K. Coulter, M. D. Ellison, J. S. Hovis, D. F. Padowitz, M. P. Schwartz, C. M. Greenlief and J. N. Russell, Jr., *Acc. Chem. Res.*, 2000, **33**, 617 and references therein.
36 F. Bacalzo-Gladden, X. Lu and M. C. Lin, *J. Phys. Chem. B*, 2001, **105**, 4368.
37 S. Haq and D. A. King, *J. Phys. Chem.*, 1996, **100**, 16 957; J. A. Rodriguez, *Surf. Sci.*, 1992, **273**, 385.
38 M. J. Frisch, G. W. Trucks, H. B. Schlegel, P. M. W. Gill, B. G. Johnson, M. A. Robb, J. R. Cheeseman, T. Keith, G. A. Peterson, J. A. Montgomery, K. Raghavachari, M. A. Al-Laham, V. G. Zakrzewski, J. V. Ortiz, J. B. Foresman, C. Y. Peng, P. Y. Ayala, W. Chen, M. W. Wong, J. L. Andres, E. S. Replogle, R. Gomperts, R. L. Martin, D. J. Fox, J. S. Binkley, D. J. Defrees, J. Baker, J. P. Stewart, M. Head-Gordon, C. Gonzalez and J. A. Pople, GAUSSIAN94, Gaussian, Inc., Pittsburgh, PA, 1995.
39 A. D. Becke, *J. Chem. Phys.*, 1993, **98**, 5648.
40 C. Lee, W. Yang and R. G. Parr, *Phys. Rev. B*, 1989, **37**, 785.
41 P. C. Hariharan and J. A. Pople, *Chem. Phys. Lett.*, 1972, **66**, 217; M. M. Francl, W. J. Pietro, W. J. Hehre, J. S. Binkley, M. S. Gordon, D. J. DeFrees and J. A. Pople, *J. Chem. Phys.*, 1982, **77**, 3654.
42 C. Gonzalez and H. B. Schlegel, *J. Chem. Phys.*, 1989, **90**, 2154.
43 J. P. Foster and F. Weinhold, *J. Am. Chem. Soc.*, 1980, **102**, 7211; A. E. Reed, L. A. Curtiss and F. Weinhold, *Chem. Rev.*, 1988, **88**, 899.
44 J. L. Armstrong, E. D. Pylant and J. M. White, *J. Vac. Sci. Technol., A*, 1998, **16**, 123.
45 M. D. Ellison, J. S. Hovis, H. Liu and R. J. Hamers, *J. Phys. Chem. B*, 1998, **102**, 8510.
46 M. D. Ellison and R. J. Hamers, *J. Phys. Chem. B*, 1999, **103**, 6243.
47 T. Shimanouchi, in *NIST Chemistry WebBook*, NIST Standard Reference Database Number 69, ed. W. G. Mallard and P. J. Linstrom, National Institute of Standards and Technology, Gaithersburg, MD, February 2000.
48 R. J. Hamers, *Nature (London)*, 2001, **412**, 489.
49 F.-J. Meyer zu Heringdorf, M. C. Reuter and R. M. Tromp, *Nature (London)*, 2001, **412**, 517.

View Online